End group effect on electrical transport through individual molecules: A microscopic study

Yongqiang Xue * and Mark A. Ratner
Department of Chemistry and Materials Research Center, Northwestern University, Evanston, IL 60208
(Dated: November 15, 2018)

The effect on molecular transport due to chemical modification of the metal-molecule interface is investigated, using as an example the prototypical molecular device formed by attaching a p-disubstituted benzene molecule onto two gold electrodes through chemically different end groups. Using a first-principles based self-consistent matrix Green's function method, we find that depending on the end group, transport through the molecule can be mediated by either near-resonant-tunneling or off-resonant-tunneling and the conductance of the molecule varies over more than two orders of magnitude. Despite the symmetric device structure of all the molecules studied, the applied bias voltage can be dropped either equally between the two metal-molecule contacts or mostly across the source (electron-injecting) contact depending on the potential landscape across the molecular junction at equilibrium.

The continuing development of molecular electronics represents the convergence of the trend of device miniaturization and the growing expertise on single-molecule manipulation through scanning nanoprobes, mechanical break junctions and supramolecular self-assembly techniques.[1] In contrast to carbon nanotubes and other inorganic semiconductor nanowires with uniform lattice structure,[2] devices based on individual organic molecules often require attaching appropriate end groups chemically different from the molecule core in order to establish stable contact to the metallic electrodes.[1] The introduction of end groups into the molecular structure has two immediate consequences: (1) it introduces molecular states that are end group-based; (2) it modifies the metal-molecule interaction through the metal-end group bond. Single-molecule devices can therefore be considered as atomic-scale heterostructured devices, [3,4] where the heterostructure can be introduced at the metal-molecule interface through the end groups or in the molecule core through appropriate molecular design techniques. The purpose of this paper is thus to elucidate the prospect of interface "engineering" of molecular transport due to chemical modification of the metal-molecule interface, through detailed microscopic study of selected single-molecule devices.

The interface "engineering" considered here is achieved through modifying the valence structure of the end group. The devices we consider are formed by attaching the p-disubstituted benzene molecule onto two semi-infinite gold electrodes through oxygen (O) and fluorine (F) end atoms and the isocyanide (C-N) end group. The device structure is shown schematically in Fig. 1. In the case of C-N end group, the end atom can be either carbon (C) or nitrogen (N). Since the hydroxyl substituent (O-H) may not deprotonate on contact with the metallic electrodes, we consider both O end atom and O-H end group in this work. For clarity in notation, we will denote the five molecules following their structure as OΦO, HOΦOH, FΦF, CNΦNC and NCΦCN (Φ stands for ben-

zene ring) respectively. The molecules chosen are thus among the smallest possible where metal-molecule interaction should have a strong effect on electrical transport, but are still representative of current experimental efforts.[1]

As the end group changes, both the energy and the charge distribution (symmetry) of the frontier molecular orbitals (occupied and unoccupied molecular orbitals energetically closest to the metal Fermi-level, -5.31 eV for gold$\langle 111 \rangle$ electrode) change, depending on the chemical difference between the end group and the core atoms. For the NCΦCN and CNΦNC molecules, both the highest-occupied-molecular-orbital (HOMO) and lowest-unoccupied-molecular-orbital (LUMO) are delocalized through the entire molecule (central benzene as well as end group) and involve mainly the P_π orbitals of carbon and nitrogen. Switching to O and F atoms, the HOMOs remain delocalized through the entire molecule, but the LUMOs become localized within the molecular core (central benzene). The HOMO-LUMO gap increases as we move from O to F (this is expected since these electron-withdrawing substituents stabilize the occupied levels). The frontier molecular states of the OΦO molecule (spin-singlet) show similar features to the phenyl dithiolate (PDT or SΦS in the present notation) molecule[3,4] due to the identical valence structure of the O and S atoms. Adding the H end atom increases the HOMO-LUMO gap of the HOΦOH molecule. Although the HOMO of the HOΦOH molecule remains delocalized over the oxygen and carbon atoms, it has little weight on the H ends which effectively reduces its coupling with the metal surface states.

Due to differences in the energy and charge distribution of the frontier molecular states, the above molecules show distinctly different behavior in the molecular response to the perturbation induced by the metal-molecule interaction and the applied bias voltage. This is investigated using a first-principles based self-consistent matrix Green's function theory which combines the

Non-Equilibrium Green's Function theory of quantum transport with an effective single-particle description of molecular junction electronic structure using density-functional theory (DFT).[3,4] The theoretical models used have been discussed extensively in our previous work,[3,4] where we presented the general theoretical approach for modeling transport through single-molecule devices within the coherent transport regime and identified two key device processes for understanding the transport characteristics of a two-terminal molecular device: the equilibrium energy-level lineup and the nonequilibrium charge/potential response to the applied bias. The same theoretical and modeling approaches are adopted here. To summarize, the gold electrodes are modeled as semi-infinite $\langle 111 \rangle$ single-crystals. Six nearest-neighbor gold atoms on each metal surface (twelve gold atoms overall) are included into the "extended molecule" where the self-consistent calculation is performed. The rest of the electrodes (with the six atoms on each surface removed) are considered as infinite electron reservoirs, whose effects are included as self-energy operators. The calculation is performed using a modified version of Gaussian98[5] using the Becke-Perdew-Wang parameterization of density-functional theory [6] and appropriate pseudopotentials with corresponding optimized Gaussian basis sets.[4,7] For comparison with our previous work and other experimental and theoretical works,[1,8] we keep the same adsorption geometry and metal surface-end group distance for all the molecules studied.[4,9] The calculation is performed at room temperature.

Following Ref. 4, we analyze the device physics of the metal-molecule-metal junction both at equilibrium and out of equilibrium. The most important quantity at equilibrium is the charge transfer between the molecule and the electrodes upon formation of the metal-molecule-metal junction, which may be understood qualitatively from the bonding configuration change across the metal-molecule interface and analyzed through the symmetry and energy of the frontier molecular orbitals. The transferred charge and the induced change in the electrostatic potential are obtained by taking the difference between the self-consistent charge/potential distribution in the equilibrium metal-molecule-metal junction and the charge/potential distribution in the isolated molecule plus the bare bimetallic junction. For the CNΦNC and NCΦCN molecules, electron densities increase on the the end atom P_π orbitals (Fig. 2). For the OΦO molecule, the overall spatial distribution of the transferred charge is similar to that of the PDT molecule (with electron density increasing on the end atom P_π orbitals but decreasing in the P_x orbitals),[4] but the magnitude of the charge transfer is larger due to the larger electronegativity of the oxygen atom which leads to a larger barrier for electron injection from the metal into the molecule (Fig. 2). Keeping the H atom reduces significantly the amount of charge transferred to the HOΦOH molecule due to the saturated H-O bond (Fig. 3). Since most of the charge transfer is to the end H and O atoms, this

leads to a large potential barrier at the H-O bonding region (Fig. 3). The FΦF molecule shows different behavior compared to the other molecules. The lowest unoccupied state is core-based, and is located about $3.8 (eV)$ above the metal Fermi-level. So the bonding configuration change is mainly realized by the charge redistribution among the occupied molecular states, leading to an electron density decrease in the fluorine-carbon σ bond and an electron density increase in the fluorine-surface bond. The magnitude of the charge transfer is much smaller than the OΦO molecule and gives rise to an electrostatic potential well instead of electrostatic potential barrier for electron injection into the molecule (Fig. 3).

The charge transfer processes and the resulting change in the electrostatic potential determine the energy-level lineup relative to the metal Fermi-level for the equilibrium molecular junction as well as low-bias conductance, which is obtained from the electron transmission characteristics at zero bias and calculated using the method of Refs. 3 and 4. The results are illustrated in Fig. 4. For comparison we have also shown the transmission characteristics of the PDT molecule. For both the CNΦNC and NCΦCN molecules, the metal Fermi-level E_F is in near-resonance with the LUMO state, which is delocalized over the entire molecule. This leads to broad transmission spectrum around E_F and large zero-bias conductance (close to the conductance quantum) due to near-resonant-tunneling through LUMO. The difference in the transmission spectrum above E_F between the two molecules is due to the difference in the energy-level spacing and broadening of the unoccupied states (the unoccupied states of CNΦCN are more closely spaced and more broadened than those of NCΦCN). The HOMO-LUMO gap of NCΦCN is also larger than that of CNΦCN, pushing the HOMO-mediated transmission peak further below E_F. For the OΦO and FΦF molecules where the end group atoms are more electron-rich, transmission at the metal Fermi-level is due to tunneling through the HOMO-LUMO gap. Although transmission through the middle of the gap is small, the HOMO of the OΦO molecule lines up much closer to the metal Fermi-level than PDT, leading to a much larger conductance. Keeping the end H atoms (HOΦOH) pushes both peaks corresponding to HOMO and LUMO down, with E_F lying slightly closer to HOMO than LUMO, which reduces the conductance of the HOΦOH junction by a factor of ≈ 100. Finally for the FΦF molecule where the end atom has the largest number of valence electrons, the LUMO instead lines up closer to the metal Fermi-level than the HOMO. Since the LUMO state of FΦF is localized on the molecule core and the HOMO state is pushed far below the metal Fermi-level (beyond the energy range plotted in Fig. 4), the zero-bias conductance is very small. As the end group changes, the conductance of the molecular junction varies by more than two orders of magnitude, from the maximum of 45.8 (μS) for the CNΦNC molecule to 0.18 (μS) for FΦF molecule.

For the device out of equilibrium, the central quan-

tity is the bias-induced charge redistribution within the molecular junction and the spatial distribution of the voltage drop, which determine the current-voltage (I-V), differential conductance-voltage (G-V) characteristics and the bias-induced modification of molecular states (the static Stark effect). The I-V and G-V characteristics are calculated self-consistently at each bias voltage and shown in Fig. 5. For the CNΦNC and NCΦCN molecules, the conductance peaks near zero-bias are due to near-resonant-tunneling through the LUMO. For the OΦO molecule, it is due to near-resonant-tunneling through the HOMO. Within the bias range considered here, both the FΦF molecule and the HOΦOH molecule are insulating due to the small tunneling probability through the HOMO-LUMO gap, leading to nearly-linear (Ohmic) I-V characteristics from $-1(V)$ to $+1(V)$. By examining the transmission characteristics as a function of the applied bias (not shown here), we find that the increase of conductance towards $\pm 2(V)$ is due to the closer alignment of the metal Fermi-levels with the LUMO for the FΦF molecule and the HOMO for the HOΦOH molecule.

Although the device structures considered here are all symmetric with respect to the exchange of the source and drain electrodes, the voltage drop across the metal-molecule-metal junction at finite bias voltage shows different behavior depending on the potential landscape throughout the equilibrium molecular junction (the voltage drop is obtained by evaluating the difference between the electrostatic potential at finite and zero biases, which obeys the boundary condition of approaching $\pm V/2$ inside the electrodes). For the CNΦNC, NCΦCN and HOΦOH molecules where there is a narrow potential barrier at the end group region but not in the molecule core at equilibrium, the voltage drops (nearly) equally between the two metal-molecule interfaces. But for the OΦO molecule where the potential barrier for electron injection is much larger and extends throughout the molecule (end group plus molecule core) region at equilibrium, most of the voltage drop occurs at the interface between the molecule and the source (electron-injecting) electrode, as illustrated in Fig. 6 for bias voltage of $2(V)$. This is readily analyzed using the concept of resistivity dipole for nonequilibrium transport systems in the presence of current flow,[4,10] where charge dipoles and correspondingly local electric fields develop in the vicinity of scattering centers (potential barriers here) to ensure the current continuity throughout the conduction system. For the OΦO molecule with a large and thick

potential barrier for electron injection, a large electrical field is required across the molecule-right electrode interface at positive bias voltage, which is sustained by a large electron deficit on the molecule side and leads to a large amount of the voltage drop across the corresponding interface (similar situation occurs at the molecule-left electrode interface at negative bias). In the case of the CNΦNC, NCΦCN and HOΦOH molecules, only a relatively small electric field is needed for electrons to penetrate a narrow barrier at the molecule-source electrode interface, so the electron redistributions around the two metal-molecule interfaces have similar magnitude and voltage drops nearly equally across the two interfaces. For the FΦF molecule where there is an electrostatic potential well in the equilibrium junction, the voltage also drops equally between the two metal-molecule interfaces due to the absence of barrier. In addition, the difference in the potential response of the molecules to the applied bias voltage leads to different behavior in the bias-induced shift of molecular levels. For the CNΦNC, NCΦCN, HOΦOH and FΦF molecules, the energy levels of HOMO and LUMO are nearly constant within the bias voltage range considered here. But for the OΦO molecule where the voltage drops mostly across the molecule-source electrode interface, the shift of the HOMO and LUMO levels follows the Fermi-level of the drain (electron-extracting) electrodes.

Discussion and Conclusion Most current experimental works on molecular electronics have focused on molecules attached to the gold electrodes through sulfur end group,[11] due to the convenient thiol-gold self-assembly scheme. In this work, we have found theoretically that depending on the end groups used, the molecules with identical molecule cores can show distinctly different behavior in their response to the perturbation induced by the metal-molecule interaction and the applied bias voltage, leading to widely different transport characteristics. Since one of the major advantages of molecular electronics is the potential to build devices with the desired properties from the bottom up, it is important to explore the feasibility of such device engineering through molecular design of interfaces. Although we are not aware of any existing single-molecule measurements that test the end group effects as reported here,[12] such tests should be plausible, in particular using the mechanical break junction techniques.[13]

[*] Author to whom correspondence should be addressed. Email: ayxue@chem.nwu.edu
[1] M.A. Reed, Proc. IEEE **97**, 652 (1999); C. Joachim, J.K. Gimzewski and A. Aviram, Nature **408**, 541 (2000) ; A. Nitzan and M.A. Ratner, Science **300**, 1384 (2003); J.R. Heath and M.A. Ratner, Phys. Today **56**(5), 43 (2003) and

references thererein.
[2] C. Dekker, Phys. Today **52**(5), 22 (1999); N.A. Melosh, A. Boukai, F. Diana, B. Gerardot, A. Badolato, P.M. Petroff, and J.R. Heath, Science **300**, 112 (2003).
[3] Y. Xue, S. Datta, and M.A. Ratner, J. Chem. Phys. **115**, 4292 (2001); Chem. Phys. **281**, 151 (2002); Y. Xue,

Ph.D. thesis, School of Electrical and Computer Engineering, Purdue University (2000); See also S. Datta, *Electron Transport in Mesoscopic Systems* (Cambridge University Press, Cambridge, 1995).

[4] Y. Xue and M.A. Ratner, Phys. Rev. B **68**, 115406 (2003); **68**, 115407 (2003).

[5] GAUSSIAN 98, Revision A.7, M. J. Frisch *et al*, Gaussian, Inc. , Pittsburgh, PA, 1998.

[6] A.D. Becke, Phys. Rev. A. **38**, 3098 (1988); M. Ernzerhof, J.P. Perdew and K. Burke, in *Density Functional Theory I*, edited by R. F. Nalewajski (Springer, Berlin, 1996).

[7] For the atoms in the molecule, we use the pseudopotential and the corresponding polarized split valence basis sets of W.J. Stevens, H. Basch and M. Krauss, J. Chem. Phys. **81**, 6026 (1984); For surface gold atom, we use the pseudopotential and the valence basis sets of P.J. Hay and W.R. Wadt, J. Chem. Phys. **82**, 270 (1985) (see Ref. 4 for details).

[8] M. Di Ventra, S.T. Pantelides, and N. D. Lang, Phys. Rev. Lett. **84**, 979 (2000); N.D. Lang and Ph. Avouris, Phys. Rev. B **64**, 125323 (2001); J.M. Seminario, A.G. Zacarias, and J.M. Tour, J. Am. Chem. Soc. **121**, 411 (1999); J. Taylor, H. Guo, and J. Wang, Phys. Rev. B **63**, 245407 (2001); P.S. Damle, A.W. Ghosh, and S. Datta, *ibid.* **64**, 201403 (2001); M. Brandbyge, J.-L. Mozos, P. Ordejón, J. Taylor, and K. Stokbro, *ibid.* **65**, 165401 (2002); J. Heurich, J.C. Cuevas, W. Wenzel, and G. Schön, Phys. Rev. Lett. **88**, 256803 (2002).

[9] In general, both the molecular and adsorption geometry will need to be determined from geometry optimization of the coupled metal-molecule-metal system, which requires a carefully characterized interface model. Since our purpose here is to illustrate the effect of interface chemistry on molecular transport, we assume that the geometry of the molecules in the junction are the same as that of the isolated molecule, which are obtained by optimization at the UBPW91/6-31G* level. The adsorption geometry is such that the end atom (the O atom in the case of OH end) sits in front of the center of the triangular gold-pad on the $\langle 111 \rangle$ surface with a end atom-surface distance of $1.9(\overset{\circ}{A})$. In the case of OH end, the O-surface distance is taken as $2.2(\overset{\circ}{A})$, while the H-surface distance is $1.9(\overset{\circ}{A})$ (the H atom lies in the plane defined by the benzene ring with an OH-OC bond angle of $108°$).

[10] R. Landauer, IBM J. Res. Develop. **1**, 223 (1957); **32**, 306 (1988); M. Büttiker, *ibid.* **32**, 317 (1988).

[11] A. Salomon, D. Cahen, S. Lindsay, J. Tomfohr, V.B. Engelkes, and C.D. Frisbie, to appear in Adv. Mater. .

[12] End group effect on the conductance of alkanethiol molecules has been reported recently by J.M. Beebe, V.B. Engelkes, L.L. Miller, and C.D. Frisbie, J. Am. Chem. Soc. **124**, 11268 (2002).

[13] J. Reichert, R. Ochs, D. Beckmann, H.B. Weber, M. Mayor and H.v. Löhneysen, Phys. Rev. Lett. **88**, 176804 (2002).
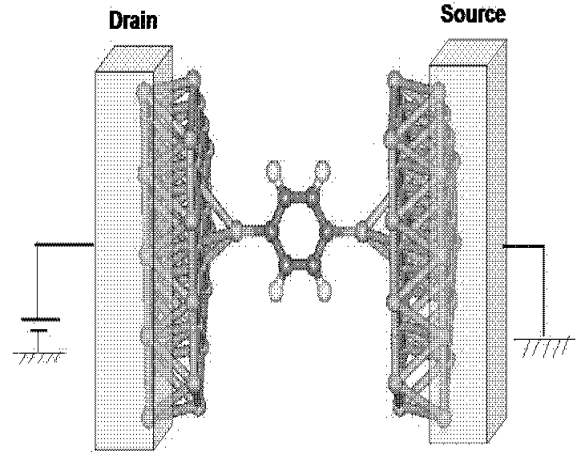
FIG. 1: (Color online) Schematic illustration of the metal-molecule-metal junction. Six gold atoms on each metal surface are included into the "extended molecule" where the self-consistent calculation is performed. The molecule can be attached onto the electrodes through chemically-different end groups.
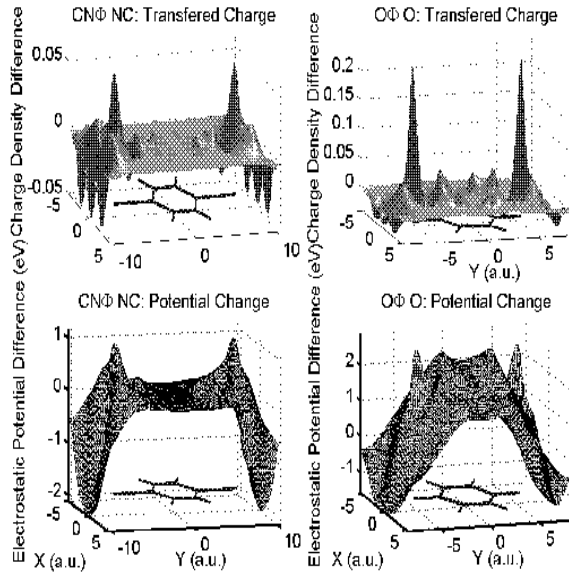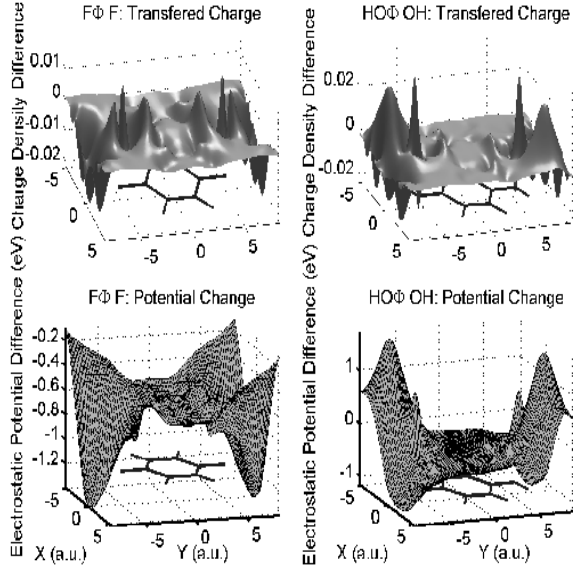
FIG. 2: (Color online) Charge transfer (in unit of $1/(\text{a.u.})^2$) and cross-sectional view of the electrostatic potential change upon the formation of the gold-CNΦNC-gold (left figure) and gold-OΦO-gold (right figure) junctions. Here the spatial distribution of the transferred electrons is plotted as a function of position in the xy-plane (defined by the benzene ring) after integrating over the z-axis. Also shown is the projection of the molecule onto the xy-plane.

FIG. 3: (Color online) Charge transfer (in unit of $1/(\text{a.u.})^2$) and cross-sectional view of the electrostatic potential change upon the formation of the gold-FΦF-gold (left figure) and gold-HOΦOH-gold (right figure) junctions. Here the spatial distribution of the transferred electrons is plotted as a function of position in the xy-plane (defined by the benzene ring) after integrating over the z-axis. Also shown is the projection of the molecule onto the xy-plane.
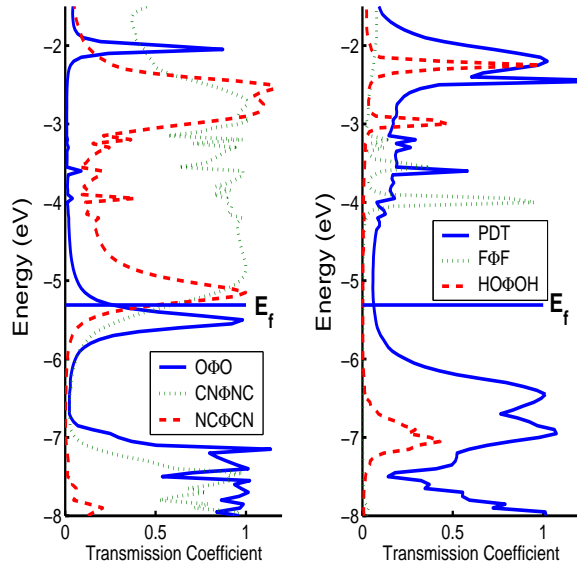
FIG. 4: Transmission versus energy characteristics of the equilibrium molecular junction (at zero bias). The horizontal lines show the location of the metal Fermi-level.
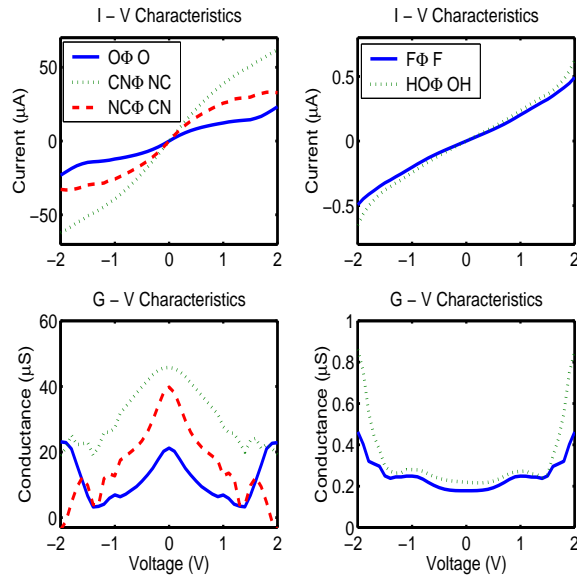

FIG. 5: Current-voltage (upper figure) and differential conductance-voltage (lower figure) characteristics of the five molecules studied in this work.
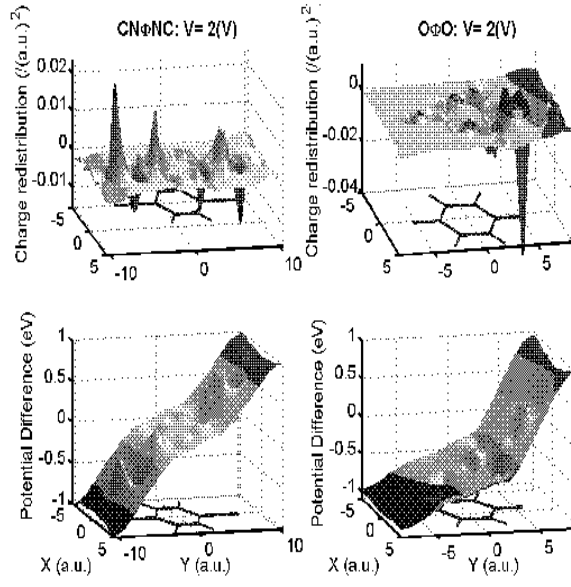
FIG. 6: (Color online) Charge redistribution and cross-sectional view of the voltage drop across the gold-CNΦNC-gold (left figure) and the gold-OΦO-gold (right figure) junction at bias voltage of $2(V)$. The transferred charge is obtained by integrating the difference in the electron density at finite and zero biases and plotted as a function of position in the xy-plane.